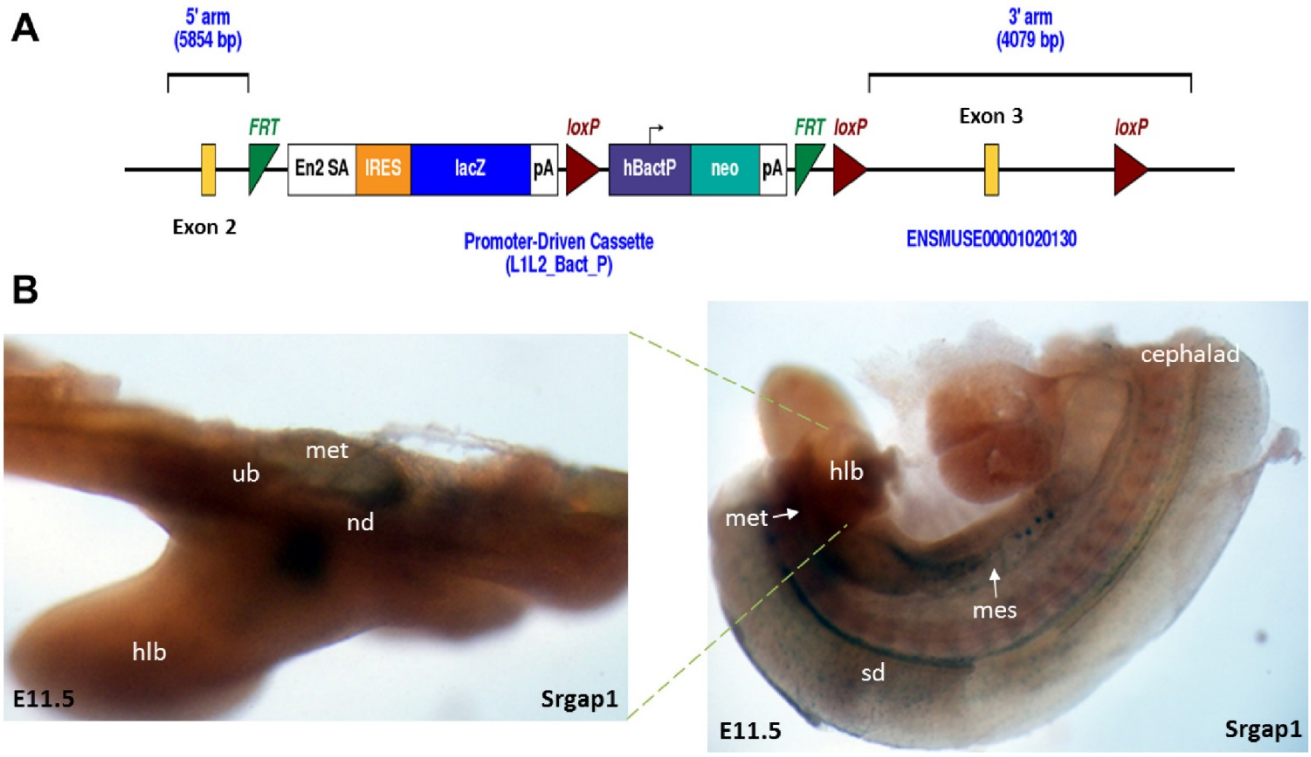

Supplementary Figure 1. *Srgap1* is expressed in early mouse developing kidney.
(A) Targeting construct for *Srgap1* with an En2SA-IRES-lacZ reporter element and a Neo-resistance cassette integrated into intron 2 of the *Srgap1* gene. The endogenous exon 2 of *Srgap1* is spliced into En2 gene splice acceptor (En2SA) that is fused with an internal ribosome entry site (IRES) and lacZ. The expression of lacZ is driven by the endogenous *Srgap1* promoter.
(B) Whole mount lacZ staining of *Srgap1* in E11.5 embryos heterozygous for the transgene. *Srgap1* promoter-driven lacZ reporter activity is detected in the E11.5 mouse developing nephrogenic mesenchyme, including the mesonephros (mes), and the metanephros (met). The left panel shows the enlarged and rotated region of the metanephros (met) and hind limb (hlb).

mes, mesonephros; met, metanephros; nd, nephric duct; pA, polyadenylation signal; sd, spinal cord; ub, ureteric bud.

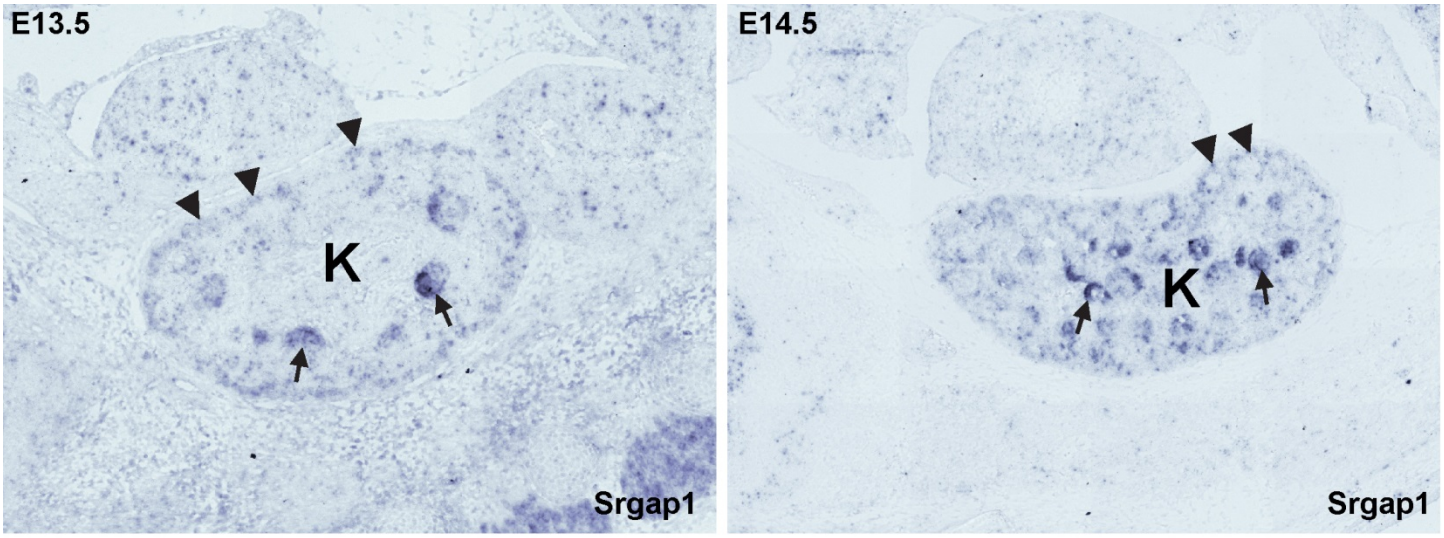

Supplementary Figure 2. *Srgap1* is expressed in mouse metanephric mesenchyme and developing glomeruli at E13.5 and E14.5.

In situ hybridization on sagittal section of mouse embryos E13.5 and E14.5 showing *Srgap1* expression in metanephric mesenchyme, including in the nephrogenic zone (black arrow heads), and in developing glomeruli (black arrows) (see also **Figure 2**). K, kidney

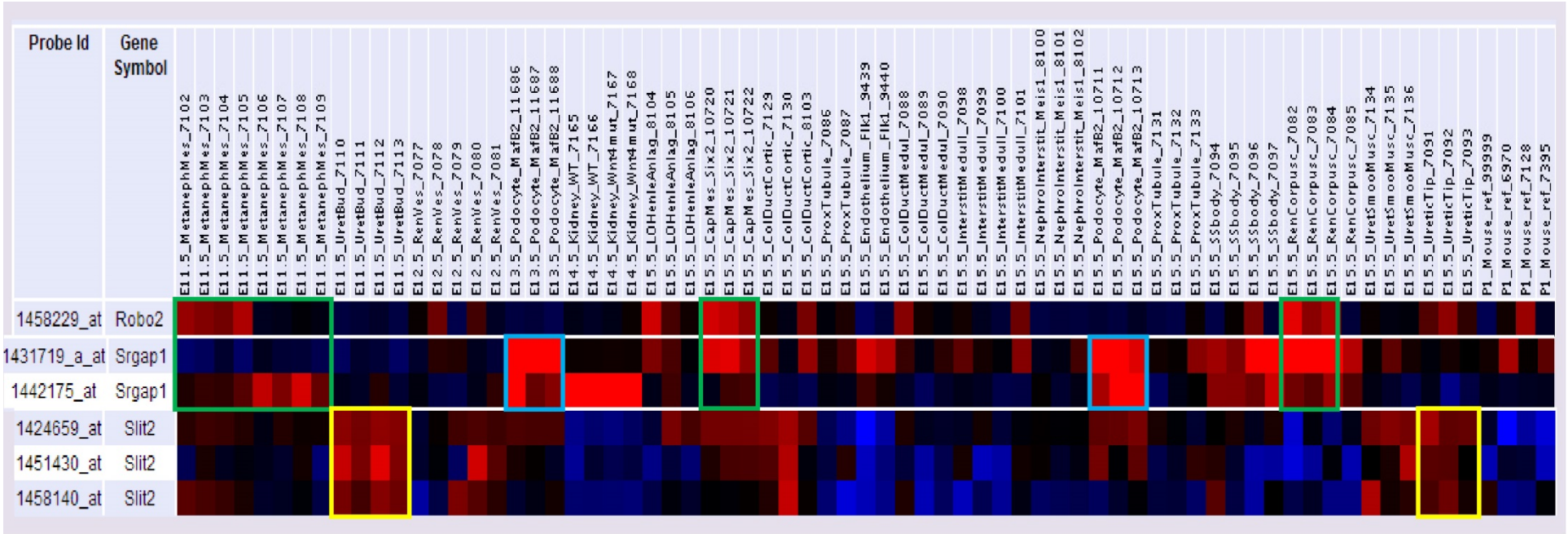

Supplementary Figure 3. *Srgap1* and *Robo2* are coexpressed in metanephric mesenchyme, cap mesenchyme, and renal corpuscle in mice at E11.5 and E15.5. *Slit2* is expressed in ureteric bud and ureteric tip at E11.5 and E15.5.

Rows represent "heat map" microarray transcription levels of for *ROBO2* (1 probe), *SRGAP1* (2 probes), and *SLIT2* (3 probes). Columns represent different nephrogenic tissues of mouse kidney E11.5 to E15.5. Above average expression appears in red colors, below average expression in blue colors. *ROBO2* and *SRGAP1* are coexpressed in metanephric mesenchyme, cap mesenchyme and renal corpuscle (green boxes). *SRGAP1* is also expressed in developing podocytes (blue boxes). SLIT2 is expressed in ureteric bud at E11.5 and ureteric tip at E15.5 (yellow boxes). Expression data was obtained from www.gudmap.org.

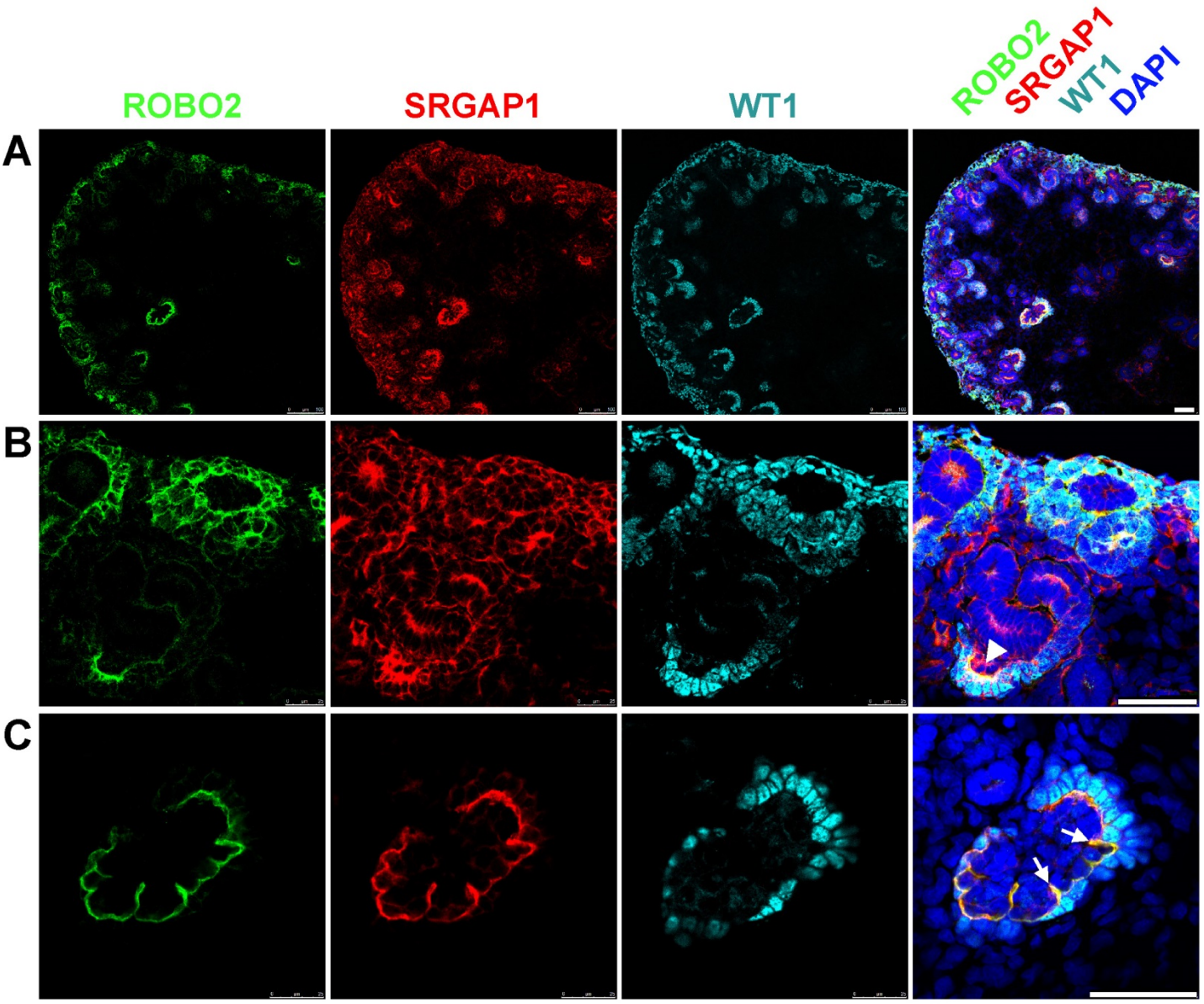

Supplementary Figure 4. SRGAP1 partially colocalizes with ROBO2 in developing podocytes. **(A-C)** In kidney sections of embryonic rats (E16.5), ROBO2 (green) and SRGAP1 (red) are present in WT1+ (green-blue) podocytes precursors in comma-shaped bodies (white arrow head) **(B)** and capillary loop stage of renal glomeruli **(C)**. Note that ROBO2 and SRGAP1 overlap at the basal side of differentiating podocytes (white arrow head and white arrows) supporting active ROBO2-SRGAP1 signaling Scale bar: 50µm.

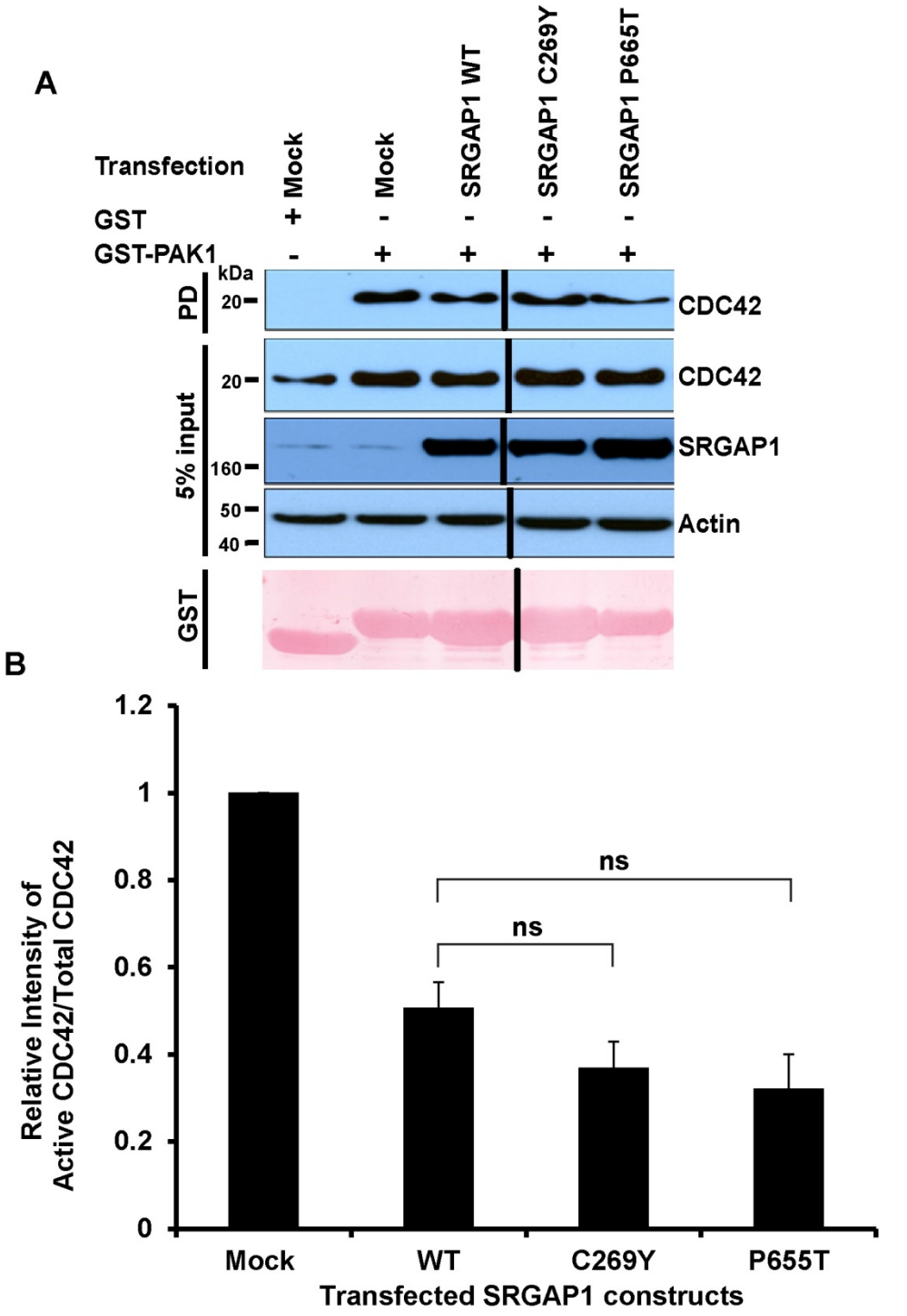

Supplementary Figure 5. Overexpression of mutant *SRGAP1* does not alter CDC42 activity in cultured HEK293T cells.

(A) Active GTP-bound CDC42 was precipitated by GST-PAK1 pulldown (PD) from HEK293T cells transfected with wildtype (WT) or mutant *SRGAP1* constructs. The efficiency of SRGAP1 transfections and 5% input control were confirmed by immunoblotting with anti-SRGAP1 and anti-actin antibodies respectively. Note that the *SRGAP1* mutants C269Y and P665T did not further reduce CDC42 activity compared to wildtype *SRGAP1*.

(B) Relative CDC42 activities (PAK1-bound CDC42/total CDC42) based on anti-CDC42 immunoblot signal intensities in (A) showing no significant difference between wildtype and mutant SRGAP1. Ratios are normalized to mock transfection.

ns, not significant (Student's t-test).

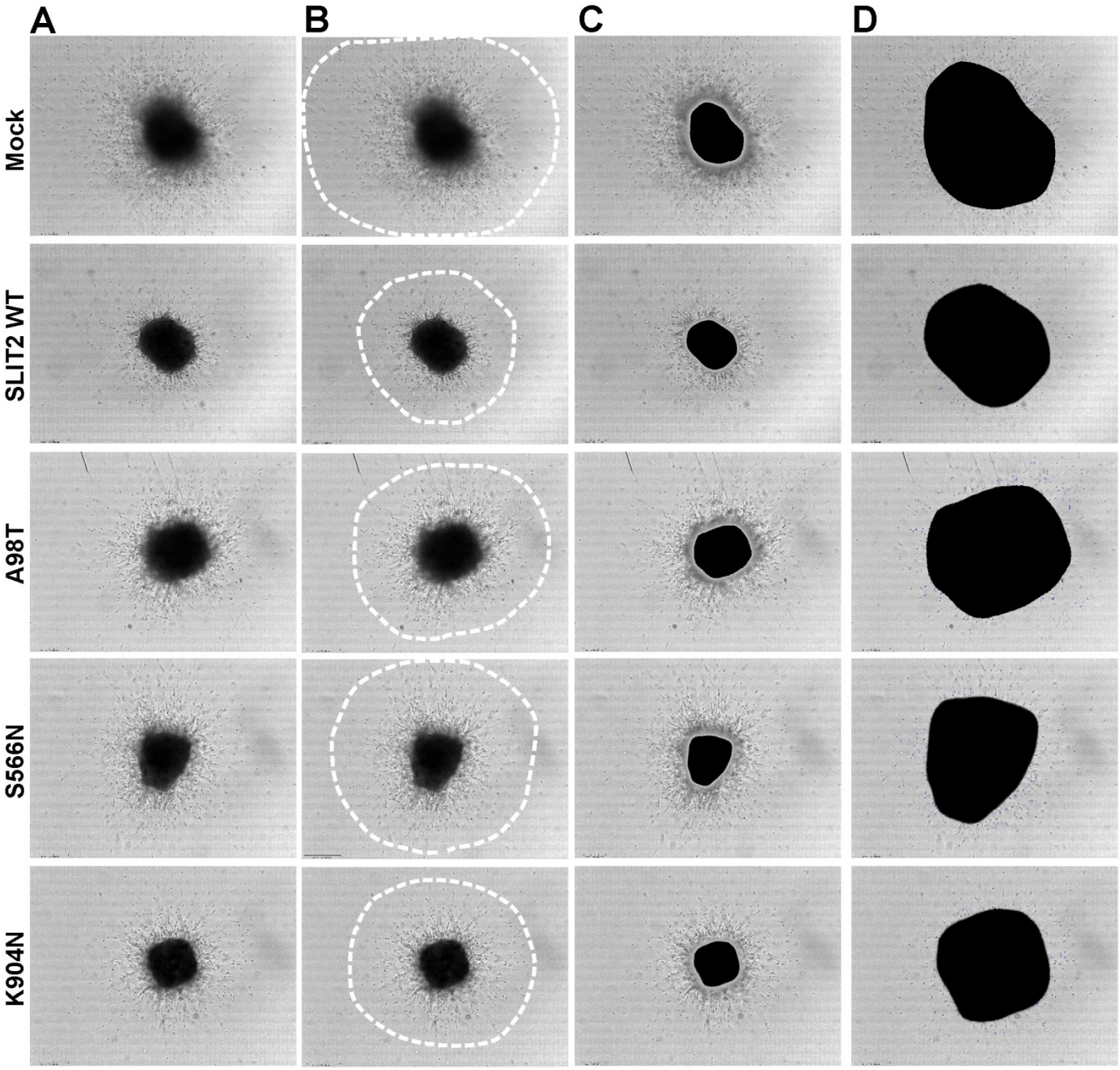

Supplementary Figure 6. Mutations in *SLIT2* detected in individuals with CAKUT reduce the chemorepulsive effect of SLIT2.

Microscopic images showing matrigel cultures of SVZa neurons after 24 hours in the presence of SLIT2 wildtype (WT) or mutant SLIT2 (A98T, S566N, K904N). SLIT2-containing media was harvested from HEK293T cells overexpressing the respective SLIT2 constructs. Mock represents SLIT2 free media. Note that wildtype SLIT2 inhibits cell migration, whereas the SLIT2 mutants have a reduced chemorepulsive effect. To quantify cell migration, migration distances were measured **(B)**. Two distances (matrigel shadow - migration outline) per obtained per quadrant. Additionally, migrated cells were counted following a masking procedure **(C and D)**, in which the central matrigel shadow was automatically selected (”Fuzzy select tool”; GIMP2 software) and filled with black **(C)**. Subsequently, the black area was proportionally enlarged by 250% while the center remained fixed **(D)**.Cells that were not covered by the enlarged matrigel shadow were defined as migrated cells and counted (”Cell counter” plug-in, ImageJ software).